The Galactic Center: Feeding and Feedback in a Normal Galactic Nucleus
Proceedings IAU Symposium No. 303, 2013
L. O. Sjouwerman, C. C. Lang & J. Ott

doi:10.1017/S1743921314001082

Diffusion of cosmic-ray electrons in the Galactic centre molecular cloud G0.13−0.13

Andrew Lehmann and Mark Wardle

Department of Physics Astronomy, and Research Center in Astronomy, Astrophysics & Astrophotonics, Macquarie University,
2109, NSW, Sydney
email: andrew.lehmann@mq.edu.au

Abstract. The Galactic center (GC) molecular cloud G0.13−0.13 exhibits a shell morphology in CS $J = (1 - 0)$, with $\sim 10^5$ solar masses and expansion speed ~ 20 km s^{-1}, yielding a total kinetic energy $\sim 10^{51}$ erg. Its morphology is also suggestive of an interaction with the nonthermal filaments of the GC arc. 74 MHz emission indicates the presence of a substantial population of low energy electrons permeating the cloud, which could either be produced by the interaction with the arc or accelerated in the shock waves responsible for the cloud's expansion. These scenarios are explored using time dependent diffusion models.

With these diffusion models, we determine the penetration of low-energy cosmic-ray electrons accelerated into G0.13−0.13 and calculate the spatial distribution of the cosmic-ray ionization and heating rates. We show that the 6.4 keV Fe Kα line emission associated with the electron population provides an observational diagnostic to distinguish these two acceleration scenarios.

We discuss the implications of our results for understanding the distinct character of clouds in the central molecular zone compared to clouds in the Galactic disk, and how GC nonthermal filaments interact with molecular clouds.

Keywords. Galaxy: center, ISM: clouds, diffusion, cosmic rays

1. Introduction

The central molecular zone (CMZ) contains many dense molecular clouds with peculiar properties. In general, they have higher temperatures, stronger magnetic fields and higher velocity dispersions than molecular clouds in the disk of the Galaxy. Constraining the causes of these properties is critical to understanding star formation processes in the CMZ.

G0.13−0.13 is a CMZ molecular cloud with a high column density of (6–7)×10^{23} cm^{-2} (Handa *et al.* 2006). It contains $\sim 10^5$ M$_\odot$ of dense molecular gas—$n(\mathrm{H_2}) = 6{\times}10^4$ cm^{-3}—and exhibits a shell morphology with expansion speed of ~ 20 km s^{-1} (Tsuboi *et al.* 1997). The cloud's morphology is also suggestive of a dynamical interaction with the nonthermal filaments of the radio arc.

Recent 74 MHz measurements of G0.13−0.13 reveal the presence of a significant population of low energy cosmic-ray (CR) electrons. These particles could be accelerated in the shock fronts of the many supernovae responsible for the shell morphology, or could be provided by the radio arc as the cloud rams into it.

This cloud is also one of the CMZ clouds correlated with diffuse 6.4 keV Fe Kα emission. These clouds have been modeled as X-ray reflection nebula tracing past energetic flashes emanating from Sgr A* (Koyama *et al.* 1996, Ponti *et al.* 2010). Alternatively, the K-shell ionizations could be due to bombardment from CR ions (Tatischeff *et al.* 2012) or CR electrons (Yusef-Zadeh *et al.* 2013). A high ionization rate from CR bombardment may

also explain the elevated temperatures of CMZ clouds (Ao *et al.* 2013) and critically affect turbulence and star formation processes.

Here we model the propagation of CR electrons through a slab of gas representing G0.13−0.13 by solving the diffusion equation. We then search for observational diagnostics by computing the ionization rate, heating rate and Fe Kα intensity due to the presence of these electrons.

2. Diffusion model

In this model, we use finite differencing to solve the 1-dimensional diffusion equation

$$\frac{\partial n}{\partial t} = Q + \kappa \frac{\partial^2 n}{\partial x^2} - \frac{\partial}{\partial p}\left(n\dot{p}\right) \tag{2.1}$$

where $n(x,p,t)dp$ is the electron density between momenta p and $p+dp$, Q is the volume injection rate of electrons, κ is the spatial diffusion coefficient and $\dot{p}$ describes the energy losses.

We use the diffusion coefficient from Chernyakova *et al.* (2011) derived by modeling a Galactic center γ-ray source:

$$\kappa = \left(10^{28}\mathrm{cm}^2\,\mathrm{s}^{-1}\right) k \left(\frac{E}{\mathrm{GeV}}\right)^{\beta}, \tag{2.2}$$

where best-fit models gave $k = 0.012$ and $\beta = 0.91$.

The NIST database for electron stopping power is used to compute bremsstrahlung and ionization losses. Synchrotron losses are negligible at these energies (10 keV–10 GeV).

We set $Q(x,p,t) = 0$ and instead model the input of electrons via boundary conditions:

$$\kappa \frac{\partial n}{\partial x}|_{x=0} = S_{\mathrm{arc}} - \frac{1}{2} v_A n(0,p,t) \tag{2.3}$$

$$\kappa \frac{\partial n}{\partial x}|_{x=L} = -S_{SNe} + \frac{1}{2} v_A n(L,p,t) \tag{2.4}$$

where v_A is the Alfvén velocity and S_{arc} and S_{SNe} are the input fluxes of electrons from the radio arc or supernovae (SNe) scenarios, both assumed to be power laws in momentum. For the arc injection scenario, the synchrotron intensity $I_\nu \propto \nu^{0.2}$ between $\nu = 74$ MHz and $\nu = 327$ MHz at a location where the cloud possibly meets the filament (Yusef-Zadeh *et al.* 2013). This gives $S \propto p^{-0.6}$ for the arc case. For electrons accelerated by supernovae shocks we use $S \propto p^{-2}$.

3. Results and discussion

Diffusion. We solve the time dependent diffusion equation until a steady state is reached, which happens for both scenarios in $t < 1000$ yrs. Plotted in Figure 1 is $E\,n(x,E,t)$ for both injection cases at $t = 100$ yrs and $t = 1000$ yrs.

The electrons from the radio arc penetrate further into the cloud than electrons from SNe. This is because the flatter input spectrum for the radio arc provides more electrons above 100 MeV, which propagate with a higher diffusion coefficient and suffer less losses than the low energy end.

Ionization rate. The CRe collisional ionization rate per H_2 molecule is

$$\zeta_{\mathrm{H}_2}(x,t) = \frac{1}{W n(\mathrm{H}_2)} \int n(x,E,t)\,\dot{E} dE \tag{3.1}$$

https://doi.org/10.1017/S1743921314001082 Published online by Cambridge University Press

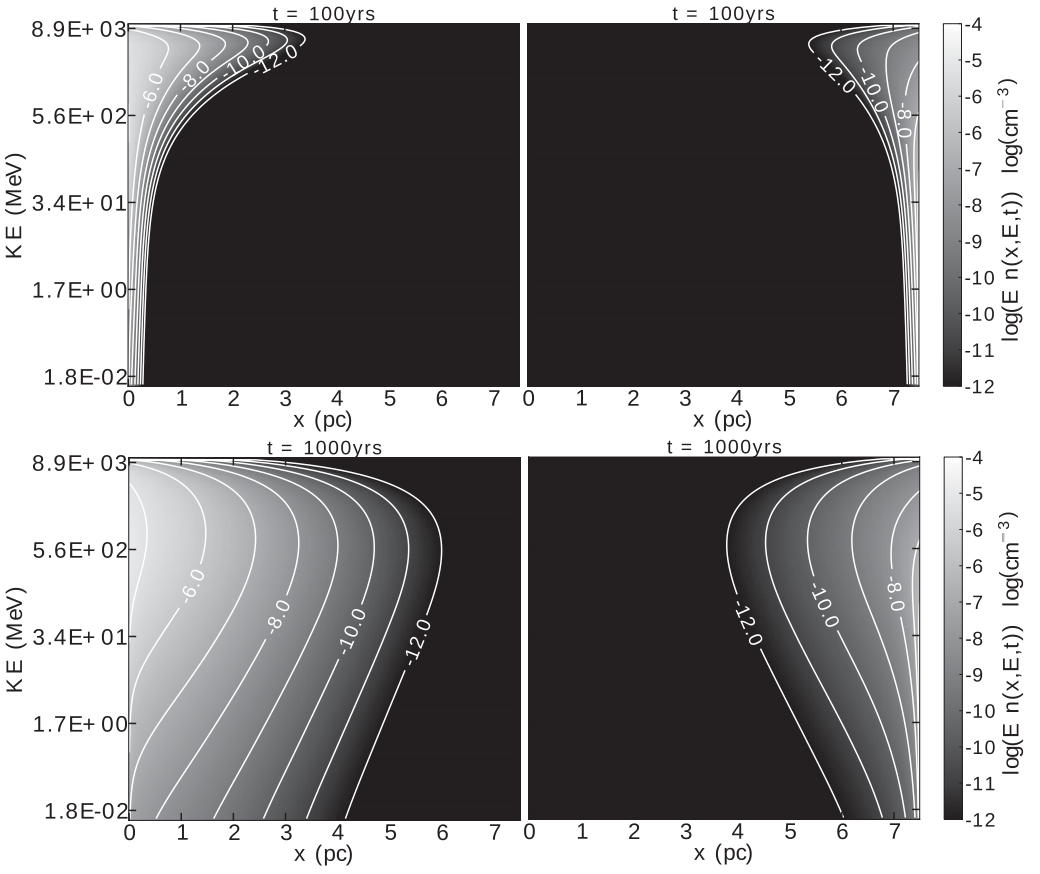

Figure 1. $E\,n(x, E, t)$ for (**left**) the radio arc injection scenario and (**right**) the SNe injection scenario at $t = 100$ yrs (**top row**) and $t = 1000$ yrs (**bottom row**).

where $W = 40.1$ eV is the average amount of energy electrons lose per ionization event (Dalgarno *et al.* 1999). The ionization rate for the two injection scenarios is shown in Figure 2 at 100 yr time intervals between $t = 100$ yrs and $t = 1000$ yrs.

Electrons from the radio arc cause ionization up to $\sim 10^{-14}$ H_2^{-1} s^{-1} and drops to the canonical galactic disk ionization rate of $\zeta_D = 10^{-17}$ H_2^{-1} s^{-1} by around 3 pc into the cloud. On the other hand, the SNe scenario only ionizes a thin ~ 0.5 pc edge above ζ_D.

An ionization rate three orders of magnitude higher than ζ_D is consistent with recent evidence of a higher rate in the CMZ (Tatischeff *et al.* 2012, Yusef-Zadeh *et al.* 2013), and also naturally explains the elevated temperatures of CMZ clouds (Ao *et al.* 2013). A heating rate is derived by noting that each ionization event eventually gives 12.4 eV of energy to heat. Equating this heating rate to the cooling rate of molecular gas at abundances twice solar (see Figure 7b in Yusef-Zadeh *et al.* 2013) implies temperatures of 30–60 K for ionization rates between 10^{-15}–10^{-14} H_2^{-1} s^{-1}.

Fe Kα emission. The Fe Kα production rate due to the presence of CR electrons is

$$q(x,t) = \frac{n(\mathrm{Fe})}{n_{\mathrm{H}}} f w_K c \int \beta \sigma_K n(x,E,t) dE \tag{3.2}$$

where σ_K is the cross section for K-shell ionization due to electron collisions, $w_K = 0.342$ is fraction of those ionizations that result in K characteristic photons, and $f = 0.822$

https://doi.org/10.1017/S1743921314001082 Published online by Cambridge University Press

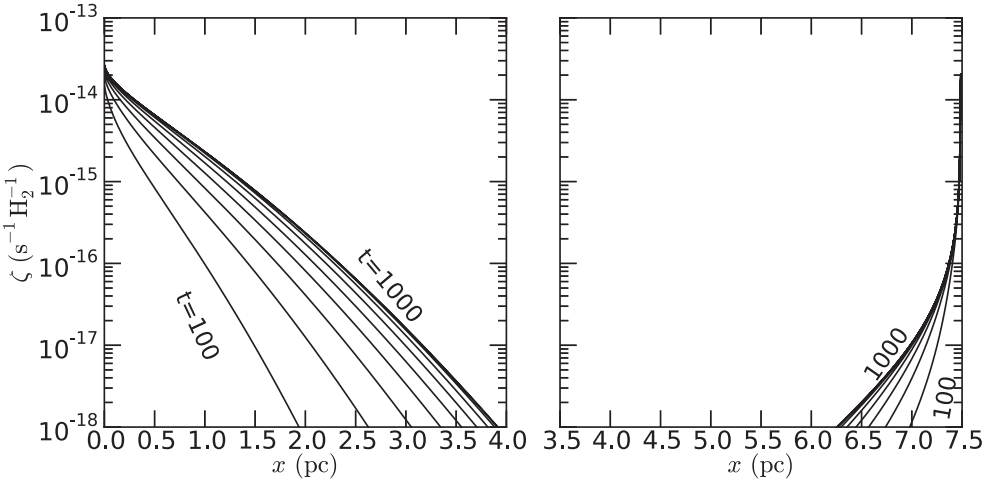

Figure 2. Ionization rate as function of position for (**left**) the arc injection scenario and (**right**) the SNe injection scenario at $t = 100, 200, \ldots, 1000$ yrs.

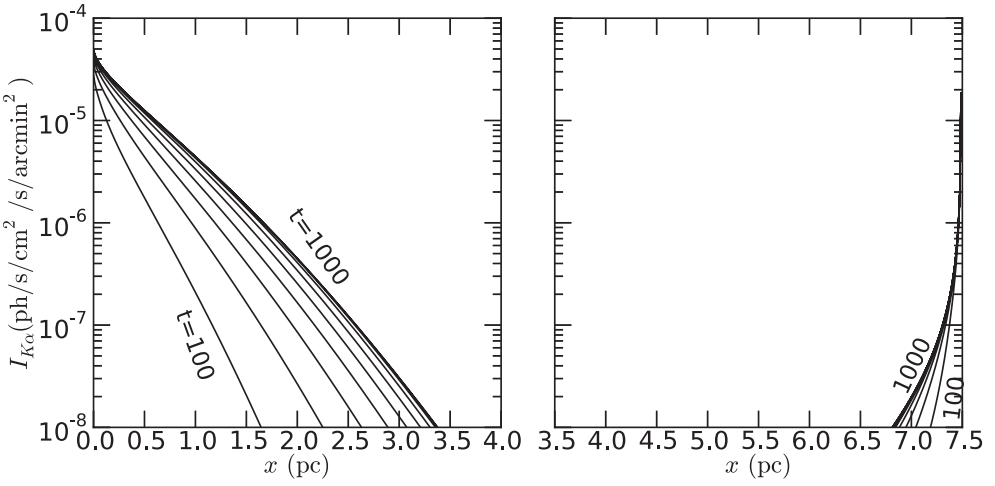

Figure 3. Fe Kα emission as function of position for (**left**) the arc injection scenario and (**right**) the SNe injection scenario at $t = 100, 200, \ldots, 1000$ yrs.

is the fraction of those that are Kα photons (Yusef-Zadeh *et al.* 2007). The intensity of this emission for the two injection scenarios is shown in Figure 3 at 100 yr time intervals between $t = 100$ yrs and $t = 1000$ yrs. For the arc injection case, the intensity is comparable to observed levels spread over a region up to 2 pc. On the other hand, the intensity from the SNe accelerated electrons is restricted to a thin region (< 0.5 pc).

4. Summary

Our preliminary results show that the ionization rate due to electrons from the radio arc reaches up to 10^{-14} H_2^{-1} s^{-1}, heats the cloud to temperatures 30–60 K two parsecs into the cloud, and causes Fe Kα emission in this region comparable to observed levels. On the other hand, electrons accelerated by supernovae ionize, heat up, and cause Fe Kα emission from only a thin (< 0.5 pc) region. This suggests that the Fe Kα emission from G0.13−0.13 is more likely to be due to electrons from the arc.

https://doi.org/10.1017/S1743921314001082 Published online by Cambridge University Press

Future work includes computing synchrotron and bremsstrahlung emission from these electron distributions, and modeling time dependent sources to possibly account for observed time dependent emission.

References

Ao, Y., Henkel, C., Menten, K. M., Requena-Torres, M. A., Stanke, T., Mauersberger, R., Aalto, S., Muehle, S., & Mangum, J. 2013, *A&A* 550, A135

Chernyakova, M., Malyshev, D., Aharonian, F., & Crocker, R., Jones D. I. 2011, *ApJ* 726, 60

Dalgarno, A., Yan, M., & Liu, W. 1999 *ApJS* 125, 237

Handa, T., Sakano, M., Naito, S., & Hiramatsu, M., Tsuboi M. 2006, *ApJ* 636, 261

Koyama, K., Maeda, Y., Sonobe, T., Takeshima, T., Tanaka, Y., & Yamauchi, S. 1996, *PASJ* 48, 249

Ponti, G., Terrier, R., Goldwurm, A., Belanger, G., & Trap, G. 2010, *ApJ* 714, 732

Tatischeff, V., Decourchelle, A., & Maurin, G. 2012, *A&A* 546, A88

Tsuboi M., Ukita, N. & Handa, T. 1997, *ApJ* 481, 263

Yusef-Zadeh, F., Muno, M., Wardle, M., & Lis, D. C. 2007, *ApJ* 656, 847

Yusef-Zadeh F., Wardle, M., Lis, D., Viti, S., Brogan, C., Chambers, E., Pound, M., & Rickert, M. 2013, *JPCA* 117, 9404